EPJ Web of Conferences **274**, 08004 (2022) https://doi.org/10.1051/epjconf/202227408004
XVth Quark Confinement and the Hadron Spectrum

Applying gauge/gravity duality to Composite Higgs models

Werner Porod[1,*]

[1]Institut für Theoretische Physik und Astrophysik, Uni. Würzburg, Campus Hubland Nord, Emil-Hilb-Weg 22, D-97074 Würzburg, Germany

Abstract. The AdS/CFT correspondence and its generalization to gauge/gravity dualities provide a very useful approach into solving strongly coupled systems. We put this at work for the strongly coupled sector of Composite Higgs models. We work out relations between masses of proposed states in Composite Higgs. As a cross check we compare these results to existing lattice calculations for which we find good agreement.

1 Introduction

Extending the AdS/CFT correspondence [1–3] to less symmetric gauge/gravity dualities has proven to be a powerful tool in describing strongly coupled gauge theories. Quarks in the fundamental representation of the gauge group can be introduced by adding probe branes [4]. This allows to study the related meson operators [5, 6]. These methods were successfully used to obtain gravity duals of chiral symmetry breaking (χSB) in confining non-Abelian gauge theories [7, 8]. A natural extension is to apply this approach to other strongly coupled theories. We focus here on composite Higgs models (CHM), see e.g. [9, 10] for reviews. These models are characterised by strongly coupled gauge theory and an underlying set of fermions dubbed hyperquarks in the following.

In composite Higgs models χSB in the fermion sector is caused by a by a strongly coupled gauge theory, similar to QCD. In this way at least four Nambu-Goldstone bosons are generated [11]. By weakly gauging part of the global chiral symmetries, four then pseudo-Nambu Goldstone bosons (pNGBs) can be placed in the fundamental representation of $SU(2)_L$ to become the complex Higgs field. The composite nature of the Higgs removes the huge level of fine tuning in the Standard Model (SM) hierarchy problem. This strong dynamics would occur at a scale of a few TeV, the expected scale for bound states. The LHC has started and, in future runs, will continue to search for such states, see e.g. [12, 13] for recent re-interpretation of existing data in the context of CHM.

We use non-conformal gauge/gravity models that explicitly include the gauge theories' dynamics through the running of the anomalous dimension γ of the hyperquark mass [14, 15]. The models are inspired by top-down models involving probe D-branes embedded into ten-dimensional supergravity. However, this is combined with a phenomenological approach and sensible guesses for the running of γ are inserted which are based on perturbation theory. With this we obtain prediction for part of the mesonic and baryonic spectrum of the theory. Here we will focus on two models, for which also lattice studies exist: an Sp(4) theory with 4 fundamental and 6 sextet Weyl quarks [16]; and an SU(4) theory with five sextet Weyl and

*e-mail: porod@physik.uni-wuerzburg.de

3 fundamental Dirac quarks [17, 18]. Further examples can be found in [15]. Both models incorporate a SM Higgs amongst their pNGBs as required by phenomenology.

The extra ingredient for which CHM were designed is the generation of the top quark's large mass, while keeping at the same time flavour changing neutral currents under control. This can be achieved by the mechanism of partial compositeness [19] to generate the top-Higgs Yukawa coupling with higher dimension operators (HDOs) from a flavour scale above the strong dynamics scale. These CHM use a mechanism where the left-handed t_L and right-handed t_R top quarks mix with baryon-like 'top partner' spin 1/2 states T_L, T_R [19]. The top partners are involved in the strong dynamics and, thus, have large Yukawa coupling to the Higgs. HDOs then mix the top and top-partner fields to generate the order one top Yukawa coupling. To model this, we first include a spinor of appropriate AdS mass into the holographic model, dual to the top partner operator in the field theory which allows us to calculate the top partners' mass. A novel technical ingredient presented in [14] is the inclusion of spinor fields into a non-supersymmetric bulk theory, for which previous results for supersymmetric probe branes have been adapted [20]. Eventually we add appropriate strongly coupled HDOs to the holographic model using Witten's double trace prescription [21]. The particular HDO chosen leads to a reduction of the top partners' mass at low energies. We demonstrate that the top Yukawa coupling can be made of order one by lowering the top partners' mass to roughly half the CHM's vector meson mass which is an important prediction for the LHC phenomenology of this model.

2 Dynamic AdS/YM

The holographic model [22] is based on the Dirac-Born-Infeld (DBI) action of a top-down model with a D7-brane embedded in a (deformed) AdS_5 geometry. The deformation is expanded to quadratic order in the embedding function X, see e.g. [23, 24]. An axial gauge field and a spinor are added similarly to AdS/QCD models [25, 26]. The model has a dimension one field for each gauge invariant operator of dimension three in the field theory. $X = Le^{i\pi}$ is dual to the complex quark bilinear or any other suitable bilinear operator, depending on the group and corresponding representation. The fluctuations of X are dual to the analog of the scalar and pseudo-scalar σ and π mesons of the theory. The gauge fields A_L^μ and A_R^μ are dual to the analogs of the vector and axial vector mesons V and A.

The gravity action of Dynamic AdS/YM is given as

$$S = \int d^5x\rho^3 \left(\frac{1}{r^2}|DX|^2 + \frac{\Delta m^2}{\rho^2}|X|^2 + \frac{1}{2g_5^2}\left(F_{L,MN}F_L^{MN} + (L \leftrightarrow R)\right) + \bar{\Psi}\left(\not{D}_{\mathrm{AAdS}} - m\right)\Psi \right). \tag{1}$$

$\not{D}_{\mathrm{AAdS}}$ is the Dirac operator evaluated on a five-dimensional asymptotically AdS (AAdS) spacetime

$$ds^2 = r^2 dx^2_{(1,3)} + \frac{d\rho^2}{r^2}\,, \tag{2}$$

in which the model lives. $r^2 = \rho^2 + L^2$ is the holographic radial direction, corresponding to the energy scale, and $dx^2_{(1,3)}$ is a four-dimensional Minkowski spacetime. The ρ and L factors in the action and metric are implemented directly from the top-down analysis of the D3/probe-D7 system. In this way an appropriate UV behaviour is ensured. Moreover, in the IR, the fluctuations know about any χSB through $L \neq 0$. The five-dimensional coupling is obtained by matching to the UV vector-vector correlator [25]

$$g_5^2 = \frac{24\pi^2}{d(R)\, N_f(R)}\,. \tag{3}$$

Here, $d(R)$ is the dimension of the quark's representation and $N_f(R)$ is the number of Weyl flavours in this representation.

The dynamics of a particular gauge theory is included through Δm^2 in eq. (1). Here we include also the hyperquark contributions to any running coupling. We set all fields to zero except for $L(\rho)$ to find the theory's vacuum with a non-zero chiral condensate. For Δm^2 a constant, the equation of motion obtained from eq. (1) reads as

$$\partial_\rho(\rho^3\partial_\rho L) - \rho\,\Delta m^2 L = 0\,. \tag{4}$$

Its solution is given by $L(\rho) = m\rho^{-\gamma} + c\rho^{\gamma-2}$, with $\Delta m^2 = \gamma(\gamma-2)$ in units of the inverse AdS radius squared. Here γ is the anomalous dimension of the hyperquark mass. The Breitenlohner-Freedman bound [27], below which an instability to χSB occurs, is given by $\Delta m^2 = -1$. The dynamics of a particular gauge theory'sis included by using its running γ to determine Δm^2. For $\gamma < 1$, we find $\Delta m^2 = -2\gamma$ and, thus, a theory triggers χSB if γ reaches $1/2$. As we do not know the true running of γ non-perturbatively, we extend the perturbative results as a function of renormalization group scale to the non-perturbative regime. We use here the two-loop anomalous dimension γ

$$\gamma = \frac{3\,C_2(R)\alpha}{2\pi} + \left(\frac{\alpha}{2\pi}\right)^2\left[\frac{3}{2}C_2(R)^2 + \frac{97}{6}C_2(R)C_2(G) - \frac{10N_f}{3}C_2(R)T(R)\right] \tag{5}$$

with a running α, which is also evaluated at the two-loop level. We solve eq. (4) numerically with our ansatz for Δm^2, using the IR boundary conditions $L(\rho = \rho_{IR}) = \rho_{\rm IR}$, $\partial_\rho L(\rho = \rho_{IR}) = 0$. These are taken from the D3/D7 system but we impose them at the scale where the hyperquarks go on mass shell. We determine the spectrum by considering fluctuations in all fields of eq. (1) about the vacuum [22].

3 Example spectra

As a first example we apply this model to the case of a CHM based on an Sp(4) gauge theory proposed in [16]. This model contains two different types hyperquarks transforming in the fundamental (F), and two-index antisymmetric (A_2) representations. The four Weyl hyperquarks in the fundamental representation feature an SU(4) flavour symmetry and the six Weyl fermions in the antisymmetric representations an SU(6) flavour symmetry. The symmetry breaking pattern is characterized by

$$\mathrm{SU}(4)\times\mathrm{SU}(6)\times\mathrm{U}(1) \to \underbrace{\mathrm{Sp}(4)}_{\mathrm{SU}(2)_L\times\mathrm{U}(1)} \times \underbrace{\mathrm{SO}(6)}_{\mathrm{SU}(3)\times\mathrm{U}(1)} \times\mathrm{U}(1) \tag{6}$$

where a combination of the U(1) factors give the hypercharge. The top partners are FA_2F bound states.

It turns out, that the A_2 fermions condense ahead of the fundamental fields, since the critical value for α where $\gamma = 1/2$ is smaller: at the level of the approximations we use the critical couplings are $\alpha_c^{A_2} = \frac{\pi}{6} = 0.53$, $\alpha_c^F = \frac{4\pi}{15} = 0.84$. It is unknown how the interplay works in detail as the breaking will occur at one scale only. Thus, we perform the AdS/YM analysis for the two fermion sectors separately, although they are linked since both flavours contribute to the running of γ down to their IR mass scale. The differences in the spectra can be interpreted as an estimate of theoretical uncertainty. We first find the $L(\rho)$ functions for the A_2 and F sectors. In a second step, we fluctuate around each embedding separately to find the spectrum where we neglect any mixing in this approximation. The results of

Table 1. AdS/$Sp(4)$ $4F, 6A_2$. Ground state spectra and decay constants for our various holographic models and comparison to lattice results - we use the subscript A_2 and F for the quantity in each of the two different representation sectors. Note here for the unquenched lattice results, which do not include the A_2 fields, we have normalized the F vector meson mass to that of the quenched computation.

	AdS/$Sp(4)$ no decouple	AdS/Sp(4) A2 decouple	AdS/Sp(4) quench	lattice [28] quench	lattice [29] unquench
$f_{\pi A_2}$	0.120	0.120	0.103	0.1453(12)	
$f_{\pi F}$	0.0569	0.0701	0.0756	0.1079(52)	0.1018(83)
M_{VA_2}	1*	1*	1*	1.000(32)	
M_{VF}	0.61	0.814	0.962	0.83(19)	0.83(27)
M_{AA_2}	1.35	1.35	1.28	1.75 (13)	
M_{AF}	0.938	1.19	1.36	1.32(18)	1.34(14)
M_{SA_2}	0.375	0.375	1.14	1.65(15)	
M_{SF}	0.325	0.902	1.25	1.52 (11)	1.40(19)
M_{TA_2}	1.85	1.85	1.86		
M_{TF}	1.13	1.53	1.79		

the holographically computed spectrum are presented in table 1 where we summarize the different cases.

Lattice data for the quenched theory have been presented in [28]. In the holographic picture the quenched theory correspond to neglecting the fermion contribution to the running. The corresponding results are presented in the forth column. We take the vector meson masses resulting from the A_2 sector to normalize the spectra The vector meson masses resulting from the fundamental hyperquarks fit the lattice data well. For the A_2 mesons, the holographic model predicts a smaller spread between the F and A_2 sectors compared to the lattice. However, within the uncertainties both pictures seem to be consistent. We find, that the holographic pion decay constants are low by 20-30%. A particular feature is, that the scalar masses dependent strongly on the strength of the running and are 10-20% lower than the corresponding lattice results. The success in the pattern suffices to make us trust changes as the theory is unquenched. We find in particular, that the gap between quantities in the A_2 and F sectors grow by 10-20% as the running between the condensation scales slows once the A_2 is integrated out, and the scalar masses fall as couplings runs less. There are also unquenched lattice results but only for the F sector [29]. Therefore, they do not shed light on the mass gap between the sectors. Nevertheless, these lattice results supports the idea that slower running reduces the scalar mass.

As a second example we take an SU(4) gauge theory which has been presented in [17, 18] for which there has been related lattice work [30, 31]. It contains five Weyl fields in the sextet A_2 representation. The condensation of the A_2 break their $SU(5)$ symmetry to $SO(5)$ and the resulting pNGBs inlcude the Higgs. Hyperquarks in the fundamental representation F are added to include top partner baryons as FA_2F states. To obtain eventually QCD one needs three Dirac spinors in the fundamental representation. When these fields condense the chiral $SU(3)_L \times SU(3)_R$ symmetry gets broken to the vector $SU(3)$ subgroup. The symmetry breaking pattern and embedding of the SM groups is given as

$$\mathrm{SU(5)} \times \mathrm{SU(3)}_L \times \mathrm{SU(3)}_R \times \mathrm{U(1)} \rightarrow \underbrace{\mathrm{SO(5)}}_{\mathrm{SU(2)}_L \times \mathrm{U(1)}} \times \underbrace{\mathrm{SU(3)}}_{\mathrm{SU(3)}} \times \mathrm{U(1)} \tag{7}$$

Due to fermion doubling problem, this model is hard to simulate on the lattice, so instead lattice work [30, 31] has focused on the case with just 2 Dirac A_2s and 2 fundamentals, which

Table 2. SU(4) theories - the spectrum in a variety of scenarios and lattice data for comparison.

	Lattice [30] $4A_2, 2F, 2\bar{F}$ unquench	AdS/$SU(4)$ $4A_2, 2F, 2\bar{F}$ no decouple	AdS/$SU(4)$ $4A_2, 2F, 2\bar{F}$ decouple	AdS/$SU(4)$ $5A_2, 3F, 3\bar{F}$ no decouple	AdS/$SU(4)$ $5A_2, 3F, 3\bar{F}$ decouple
$f_{\pi A_2}$	0.15(4)	0.0997	0.0997	0.111	0.111
$f_{\pi F}$	0.11(2)	0.0949	0.0953	0.0844	0.109
M_{VA_2}	1.00(4)	1*	1*	1*	1*
M_{VF}	0.93(7)	0.933	0.939	0.890	0.904
M_{AA_2}		1.37	1.37	1.32	1.32
M_{AF}		1.37	1.37	1.21	1.23
M_{SA_2}		0.873	0.873	0.684	0.684
M_{SF}		1.03	1.02	0.811	0.798
M_{JA_2}	3.9(3)	2.21	2.21	2.21	2.21
M_{JF}	2.0(2)	2.07	2.08	1.97	2.00
M_{TA_2}	1.4(1)	1.85	1.85	1.85	1.85
M_{TF}	1.4(1)	1.74	1.75	1.65	1.68

allows consideration of the unquenched case. Our results are summarized in table 2 where we also include lattice data from [30]. The holographic approach, for which we adjusted the fermion content to match the lattice, and the lattice agree in the vector meson sector. However, the pion decay constants lie close to or just below the lower lattice error bar. In addition we obtain masses that have not been computed on the lattice. More importantly, we can easily move to the original hyperquark content for the CHM of [17, 18]. We see that the extra hyperquarks slow the running between the A_2 and F mass scales and reduce the F sector masses by about 10%. Similar to the previous model, the scalar masses again fall by about 20% as a consequence of the slower running.

4 Top partners

In the two models presented above, the top partners are FA_2F states, spin-1/2 baryons of the strong dynamics. We describe them by a spinor fluctuating in AdS [32] which is dual to the baryon operator. From the action in eq. (1), one derives a second order wave equation for the spinor based on [20]. The main features can be summarized as follows: states with $\Delta = 9/2$, appropriate for three-quark states, have an AdS mass $m = 5/2$. The corresponding spinor can be written as eigenstates of the γ_ρ projector, with $\gamma_\rho\psi_\pm = \pm\psi_\pm$. The equation of motion then splits into two copies of the dynamics, for ψ_+ and for ψ_-, with explicit relations between the solutions [20]. The full solutions are found numerically, see e.g. [15] for further details. We again use IR boundary conditions imported from the D7 probe case: $\psi_+(\rho = L_{IR}) = 1$ and $\partial_\rho\psi_+(\rho = L_{IR}) = 0$.

This allows the computation of the baryon masses for three-fermion states associated with a particular background $L(\rho)$. We note, that we wish to set $O = FA_2F$ which is a mixed state. Thus,in principle the computation should take into account that the A_2 and F states have distinct $L(\rho)$. We simplify this by using one $L(\rho)$, either that for F or A_2, which assumes the flavours are degenerate. The two choices give predictions for the baryon masses, M_{TA_2} and M_{TF} at the bottom of table 2 and we expect that the correct mass lies between these two values. Compared to the lattice data our estimate is 25% high, but still within the uncertainties.

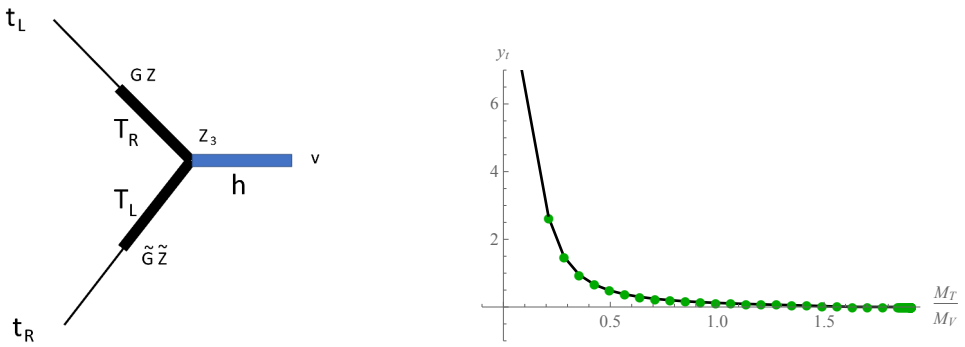

Figure 1. Left: The top Yukawa coupling (y_t) vertex diagram. **Right:** Yukawa coupling as function of the top partner mass in the A_2 sector of the SU(4) gauge theory (with $g = \tilde{g} = 1$).

The top mass is generated by the diagram in the left part of figure 1. The Z factors shown are structure functions that depend on the strong dynamics. g^2/Λ^2 and the corresponding tilded vertex, which we won't distinguish in the following, are the dimensionful couplings of the HDOs. They mix the top and top partners of the form $\bar{t}_{L/R}\mathcal{O}$. For the computation of the Z_3 factor we would need a cubic term in eq. (1). The corresponding coupling is not determined in the bottom-up approach. Nevertheless, on dimensional grounds, a sensible holographic estimate for the Z_3 factor is a weighted integral over the scalar and baryon wave functions [15]:

$$Z_3 \simeq \int d\rho\, \rho^3 \frac{\psi_T^2 \partial_\rho \sigma_h}{(\rho^2 + L^2)^2}\,. \tag{8}$$

Similarly one finds for the two other factors

$$Z \simeq \tilde{Z} \simeq \int d\rho\, \rho^3 \partial_\rho \psi_B\,. \tag{9}$$

σ_h and ψ_T are ρ dependent holographic wavefunctions for the scalar meson and baryon, respectively. The top Yukawa coupling,

$$y_t = \frac{g^2 Z\, \tilde{g}^2 \tilde{Z}\, Z_3}{M_T^2\, \Lambda^4}\,, \tag{10}$$

is inversely proportional to the top partner mass squared. It is proportional to the Z_3 and $Z/\tilde{Z}$ factors. We have computed y_t in both models. Setting a cut off Λ roughly 6 times the vector meson mass, we find the top Yukawa coupling is only of order 10^{-2} which is clearly far below the required value of 1. This is the standard problem when trying to generate the top mass as it is suppressed both by the HDO scale Λ and top partner mass squared.

A solution to this is to enhance y_t by including a further HDO [14] given by

$$\mathcal{L}_{\text{HDO}} = \frac{g_T^2}{\Lambda^5} |F A_2 F|^2\,. \tag{11}$$

This is directly a shift in its mass as the operator FA_2F becomes the top partner. We use Witten's double trace prescription [21] to include this holographically: the vacuum expectation value $\langle FA_2F\rangle$ contributes to the source via $\mathcal{J} = \frac{g_T^2}{\Lambda^5}\langle FA_2F\rangle$ once the contribution given in eq. (11) is turned on. The HDO in eq. (11) can indeed be used to reduce the top partner's

mass as was shown in a more formal setting [20]. For small g_T the effect is small and scales linearly, but after a critical value the effect is much larger.

This change of the top partner masses affects the computation of the top Yukawa [14, 15]. As the top partner's mass changes, so do the Z factors in eqs. (8) and (9). The HDO in eq. (11) plays an important role because it induces a sizeable non-normalizable piece in the UV holographic wave function of the top partner. The corresponding integrals in the normalization factors for the state, which enter directly in the expressions for the Z factors, are more dominated by the UV part of the integral. Moreover, also the overlap between different states can change substantially . We show the dependence of the top Yukawa coupling on the top partner mass to the right of figure 1. We see that the top Yukawa increases as the top partner's mass decreases and can become of order 1 when the top partner mass is about half of the vector meson mass.

5 Conclusions

We have shown that gauge/gravity duality methods are a powerful tool for obtaining sensible estimates for masses of the bound states in strongly coupled theories relevant to composite Higgs models., The AdS/YM framework presented here allows for fast computations. Moreover, the fermion content of the model considered can be changed in a simple way. We have in particular considered two examples for which also lattice data are available and find reasonable agreement taking into account the uncertainties on both side. Further examples can be found in ref. [15]. Moreover, we have seen that in order to obtain a reasonable top Yukawa coupling, one has to take into account higher dimensional operators which impact in particular on the ratio top partner mass over vector meson mass [14, 15].

Acknowledgements

I would like to thank R. Abt, J. Erdmenger, N. Evans, Y. Liu and K.S. Rigatos for fruitful and interesting discussions.

References

[1] J.M. Maldacena, Adv. Theor. Math. Phys. **2**, 231 (1998), hep-th/9711200
[2] E. Witten, Adv. Theor. Math. Phys. **2**, 253 (1998), hep-th/9802150
[3] S.S. Gubser, I.R. Klebanov, A.M. Polyakov, Phys. Lett. B **428**, 105 (1998), hep-th/9802109
[4] A. Karch, E. Katz, JHEP **06**, 043 (2002), hep-th/0205236
[5] M. Kruczenski, D. Mateos, R.C. Myers, D.J. Winters, JHEP **07**, 049 (2003), hep-th/0304032
[6] J. Erdmenger, N. Evans, I. Kirsch, E. Threlfall, Eur. Phys. J. A **35**, 81 (2008), arXiv:0711.4467
[7] J. Babington, J. Erdmenger, N.J. Evans, Z. Guralnik, I. Kirsch, Phys. Rev. D **69**, 066007 (2004), hep-th/0306018
[8] M. Kruczenski, D. Mateos, R.C. Myers, D.J. Winters, JHEP **05**, 041 (2004), hep-th/0311270
[9] G. Cacciapaglia, C. Pica, F. Sannino, Phys. Rept. **877**, 1 (2020), arXiv:2002.04914
[10] G. Panico, A. Wulzer, *The Composite Nambu-Goldstone Higgs*, Vol. 913 (Springer, 2016), arXiv:1506.01961

[11] M.J. Dugan, H. Georgi, D.B. Kaplan, Nucl. Phys. B **254**, 299 (1985)
[12] G. Cacciapaglia, T. Flacke, M. Kunkel, W. Porod, L. Schwarze (2022), arXiv:2210.01826
[13] G. Cacciapaglia, T. Flacke, M. Kunkel, W. Porod, JHEP **02**, 208 (2022), arXiv:2112.00019
[14] J. Erdmenger, N. Evans, W. Porod, K.S. Rigatos, Phys. Rev. Lett. **126**, 071602 (2021), arXiv:2009.10737
[15] J. Erdmenger, N. Evans, W. Porod, K.S. Rigatos, JHEP **02**, 058 (2021), arXiv:2010.10279
[16] J. Barnard, T. Gherghetta, T.S. Ray, JHEP **02**, 002 (2014), arXiv:1311.6562
[17] G. Ferretti, JHEP **06**, 142 (2014), arXiv:1404.7137
[18] G. Ferretti, JHEP **06**, 107 (2016), arXiv:1604.06467
[19] D.B. Kaplan, Nucl. Phys. B **365**, 259 (1991)
[20] R. Abt, J. Erdmenger, N. Evans, K.S. Rigatos, JHEP **11**, 160 (2019), arXiv:1907.09489
[21] E. Witten (2001), hep-th/0112258
[22] T. Alho, N. Evans, K. Tuominen, Phys. Rev. D **88**, 105016 (2013), arXiv:1307.4896
[23] R. Alvares, N. Evans, K.Y. Kim, Phys. Rev. D **86**, 026008 (2012), arXiv:1204.2474
[24] J. Erdmenger, N. Evans, M. Scott, Phys. Rev. D **91**, 085004 (2015), arXiv:1412.3165
[25] J. Erlich, E. Katz, D.T. Son, M.A. Stephanov, Phys. Rev. Lett. **95**, 261602 (2005), hep-ph/0501128
[26] L. Da Rold, A. Pomarol, Nucl. Phys. B **721**, 79 (2005), hep-ph/0501218
[27] P. Breitenlohner, D.Z. Freedman, Annals Phys. **144**, 249 (1982)
[28] E. Bennett, D.K. Hong, J.W. Lee, C.J.D. Lin, B. Lucini, M. Mesiti, M. Piai, J. Rantaharju, D. Vadacchino, Phys. Rev. D **101**, 074516 (2020), arXiv:1912.06505
[29] E. Bennett, D.K. Hong, J.W. Lee, C.J.D. Lin, B. Lucini, M. Piai, D. Vadacchino, JHEP **12**, 053 (2019), arXiv:1909.12662
[30] V. Ayyar, T. Degrand, D.C. Hackett, W.I. Jay, E.T. Neil, Y. Shamir, B. Svetitsky, Phys. Rev. D **97**, 114505 (2018), arXiv:1801.05809
[31] V. Ayyar, T. DeGrand, M. Golterman, D.C. Hackett, W.I. Jay, E.T. Neil, Y. Shamir, B. Svetitsky, Phys. Rev. D **97**, 074505 (2018), arXiv:1710.00806
[32] I. Kirsch, JHEP **09**, 052 (2006), hep-th/0607205